Rescaling the Dynamics of Evaporating Drops

C. Poulard,† G. Guéna,† A. M. Cazabat,*,† A. Boudaoud,‡ and M. Ben Amar‡

Collège de France, 11 place Marcelin Berthelot, 75231 Paris Cedex 05, France, and Laboratoire de Physique Statistique de l'Ecole Normale Supérieure, 24 rue Lhomond, 75231 Paris Cedex 05, France

Received February 15, 2005. In Final Form: June 24, 2005

The dynamics of evaporation of wetting droplets is investigated experimentally in an extended range of drop sizes to provide trends relevant for a theoretical analysis. A model is proposed, which generalizes Tanner's law in the presence of evaporation. A qualitative agreement is obtained, which represents a first step toward the solution of a very old, complex problem.

1. Introduction

For practical reasons, the evaporation of drops, either free in aerosols[1,2] or deposited on fibers[3−5] or flat substrates[6−13] has been extensively studied in the past and is still the subject of many investigations.[14−19] While the most recent studies deal with the structure of deposits from evaporating colloidal dispersions,[20−22] the mere problem of the dynamics of evaporation of pure liquid drops on flat, smooth, and horizontal substrates is not yet fully understood. The main difficulty is encountered in the complete wetting case, where the contact line moves freely on the substrate, either advancing or receding on it.[23−25] From the theoretical point of view, two singularities have to be coped simultaneously, with one associated with the well-known problem of a moving contact line and the second associated with the specific behavior of the evaporation flux at the edge of the drop. From the experimental point of view, the dynamics reveals to be rather sensitive to the surface energy, which is usually not the case in complete wetting. Actually, for nonvolatile wetting liquids, the dynamic properties depend only logarithmically on the spreading parameter.[25]

The present paper brings a new piece toward a better understanding of the dynamics of evaporation of completely wetting drops of pure liquids on smooth substrates.

Summary of Our Previous Findings.[17−19] To address the basic questions without too much interference of complex physicochemical behavior, we chose to study alkane drops evaporating on oxidized silicon wafers under normal atmosphere. When properly cleaned, the amorphous silica surface is hydrophilic, ensuring complete wetting, and the underlying silicon provides the high optical contrast required for interferometric measurements. A proper choice of alkanes, from hexane to nonane, allows us to vary the evaporation rate by a factor of 35 while retaining the assumption of a diffusion-controlled, quasistationary evaporation process, at least for the main part of the drop's life.[21] A consequence is that the laplacian Δc of the concentration c of the evaporating compound in the atmosphere is $\Delta c = 0$.[26]

This assumption is well-obeyed in aerosols and leads to simple laws for the radius (or the area) of the evaporating spheres: if t_0 is the time where the drop disappears, then the radius scales with time t as $\sqrt{t_0 - t}$.[27−28] The square-root dependence basically results from $\Delta c = 0$ and is therefore quite robust. For sessile wetting drops, the presence of a third phase and a contact line obviously makes the situation more complex. However, during the receding motion, the radius of the wetted spot is found experimentally to scale as $(t_0 - t)^y$, where y is close to 0.5, more precisely between 0.44 for nonane and 0.48 for hexane. The quality of the fit is excellent over the whole retraction.

Therefore, the dynamics of the radius is essentially defined by general trends, and the laws for sessile drops differ only by higher order terms from the "diffusive dynamics" of spherical ones.

* To whom correspondence should be addressed. Telephone: 33-1-44-27-10-81. Fax: 33-1-44-27-10-82. E-mail: anne-marie.cazabat@college-de-france.fr.

† Collège de France.

‡ Laboratoire de Physique Statistique de l'Ecole Normale Supérieure.

(1) Roth, N.; Frohn, A. *Dynamics of Droplets*; Springer: New York, 2000.

(2) Roth, N.; Anders, K.; Frohn, A. Size and evaporation rate measurements of optically levitated droplets. In *Proceedings of the 3rd International Congress on Optical Particle Sizing*; 1993; pp 371−377.

(3) Topley, B.; Whytlaw-Gray, R. *Philos. Mag.* **1927**, *4*, 873.

(4) Houghton, H. G. *Physics* **1933**, *4*, 419.

(5) Ranz, W. E.; Marshall, W. R. *Chem. Eng. Prog.* **1952**, *48*, 173.

(6) Morse, H. W. *Proc. Am. Acad. Sci.* **1910**, *45*, 363.

(7) Ehrhard, P.; Davis, S. H. *Fluid Mech., J.* **1991**, *229*, 365.

(8) Anderson, D. M.; Davis, S. H. *Phys. Fluids* **1995**, *7*, 248.

(9) Hocking, L. M. *Phys. Fluids* **1995**, *7*, 2950.

(10) Bourguès-Monnier, C.; Shanahan, M. E. *Langmuir* **1995**, *11*, 2820.

(11) Shanahan, M. E. *Langmuir* **1995**, *11*, 1041.

(12) Birdi, K. S.; Vu, D. T.; Winter, A. *J. Phys. Chem.* **1989**, *93*, 3702.

(13) Betterton, M.; Brenner, M.; Stone, H. Private communication.

(14) Deegan, R. D. *Phys. Rev. E* **2000**, *61*, 475.

(15) Morris, S. J. S. *Fluid Mech., J.* **2001**, *432*.

(16) Hu, H.; Larson, R. G. *J. Phys. Chem. B* **2002**, *106*, 1334.

(17) Cachile, M.; Bénichou, O.; Cazabat, A. M. *Langmuir* **2002**, *18*, 7985.

(18) Cachile, M.; Bénichou, O.; Poulard, C.; Cazabat, A. M. *Langmuir* **2002**, *18*, 8070.

(19) Poulard, C.; Bénichou, O.; Cazabat, A. M. *Langmuir* **2003**, *19*, 8828.

(20) Deegan, R. D.; Bakajin, O.; Dupont, T. F.; Huber, G.; Nagel, S. R.; Witten, T. A. *Nature* **1997**, *389*, 827.

(21) Deegan, R. D.; Bakajin, O.; Dupont, T. F.; Huber, G.; Nagel, S. R.; Witten, T. A. *Phys. Rev. E* **2000**, *62*, 757.

(22) Parisse, F.; Allain, C. *Langmuir* **1996**, *13*, 3598.

(23) Blake, T. D. AIChE spring meeting; New Orleans, LA, 1988; paper I.a.

(24) Pomeau, Y. *C. R. Acad. Sci. Paris* **2000**, *328*, 411.

(25) de Gennes, P. G. Wetting: Statics and dynamics. *Rev. Mod. Phys.* **1985**, *57*, 827.

(26) Maxwell, J. C. Diffusion, collected scientific papers. *Encyclopedia Britannica*, Cambridge, U.K., 1877.

(27) Langmuir, I. Evaporation of small spheres. *Phys. Rev.* **1918**, *12*, 368.

(28) Fuchs, N. A. *Evaporation and Growth in Gaseous Media*; Bradley, R. S., Ed.; Pergamon Press: Elmsford, NY, 1959.

10.1021/la050406v CCC: $30.25
Published on Web 08/06/2005

In contrast, the contact angle is very sensitive to all of the parameters involved: the volatility of the liquid, the surface energy of the substrate, and more insidiously, the thermal conductivity of the phases and the velocity of the moving contact line. For nonvolatile wetting liquids, the advancing dynamic contact angle depends on the contact line velocity and the receding one is 0, with a thin film being left on the substrate. In the present case, the receding contact angle does not vanish but typical values are small.[17−19] The experiments show that, in the main part of the retraction, the contact angle decreases slowly and scales acceptably as $(t_0 - t)^x$, where x is positive and small. When the assumption of a diffusion-controlled, quasi-stationary evaporation process and the assumption that the drop is a spherical cap are combined, one may predict that x and y are linked by $2y + x = 1$, which is actually well-obeyed. Without surprise, x depends upon the difference between y and the value 0.5 of the dynamics of free drops.

However, no prediction is available still for the precise value of y (or x) and for the dependence of the contact angle with liquid volatility and substrate energy. Moreover, the behavior of the contact angle, either at the beginning of the retraction or at the very end of the drop life,[19] differs significantly from the slow decrease mentioned above. Therefore, further experiments are required to guide the theoretical analysis. From this point of view, sensitive parameters as contact angle and drop profiles are precious indicators, although difficult to work with.

2. New Experiments

Two types of experiments have been performed. In the first one, the experimental setup is the same as in the previous papers.[17−19] The dynamics of wetting drops of volatile alkanes is followed under a microscope, in normal atmosphere, with protections against air draft. The radius and contact angle are recorded versus the elapsed time both during spreading (advancing motion) and retraction (receding motion). The data are conveniently plotted versus $t_0 - t$, where t_0 is the time where the drop disappears. In contrast to the previous studies, the volume of the drop is varied significantly and the crossover between spreading and retraction is investigated.

The study of the crossover has to be done carefully. The magnification needed for measuring the angle from equal-thickness interference fringes prevents us frommeasuring the radius simultaneously without manipulation of the objectives, which is out of question because it is enough to change the contact angle significantly. The radius is calculated from the visible part of the contact line, and the result is checked against an experimental curve (maximum radius versus initial volume of the drop), obtained independently and used as a "standard" (Figure 1).

The aim of the second setup is rather to spot behaviors that are not consistent with the various assumptions used in the analyses. A parallel monochromatic beam is sent normal to the drop. The silicon wafer is a plane mirror, and the reflected light is analyzed (Figure 2). (i) Part 1 of the beam does not meet the drop. We shall not discuss it further. (ii) Part 2 is reflected by the drop surface. (iii) Part 3 passes through the drop, is reflected on the silicon, then goes back. Therefore, the drop acts as both a mirror (2) and a lens, which is crossed twice (3). The contact angle is small, a few degrees at most. The two beams are received on a screen, directly or through a lens. It is possible to insert masks on the incident beam to illuminate a fraction of the drop, either at the center or in the vicinity of the edge. From the points of convergence of the beam (3) and from the size of the various spots on the screen, information on the curvature of the drop, then the radius, and the contact angle is obtained.

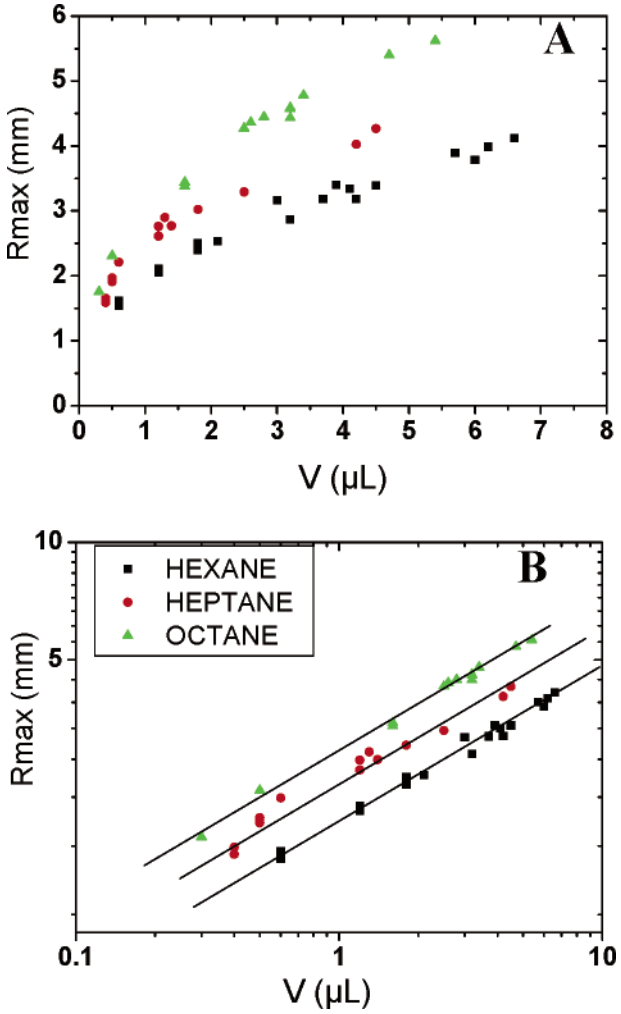

Figure 1. (A) Linear plot of maximum radii versus initial volume for different alkanes. (B) Log−log representation of A. The lines with slope ~0.4 are guides for the eyes.

If the drop is a spherical cap, the results are the same with or without masks and the point of convergence of the beam (3) on the axis is well-defined (see Figure 2).

If the drop is not a spherical cap, because of gravity or any surface tension gradient, the results are different. If the drop is flatter, the lens with the mask on the center has a shorter focal length and conversely.

With the mask on the center, the convergence of the beam (3) is well-defined and allows us to deduce R/θ in the vicinity of the contact line. In contrast, with a hole of radius $\rho = 2$ mm, the light is distributed on a small segment of the optical axis. The shortest length of convergence corresponds to the part of the drop located approximately at a distance ρ from the center and allows us to calculate $\rho/\theta_{(r=\rho)}$. The longest length corresponds to the curvature at the center, but the difference is less than 10% and will be ignored in the following.

The experiment provides a useful global picture of the behavior of the evaporating drop and information on the shape, which is quite important. As a matter of fact, the complete profile can be obtained from interference fringes only at the very end of the drop life.

Summary of the Results. First, the radius R of drops of nonane (Figure 3a), octane (Figure 3b), heptane (Figure

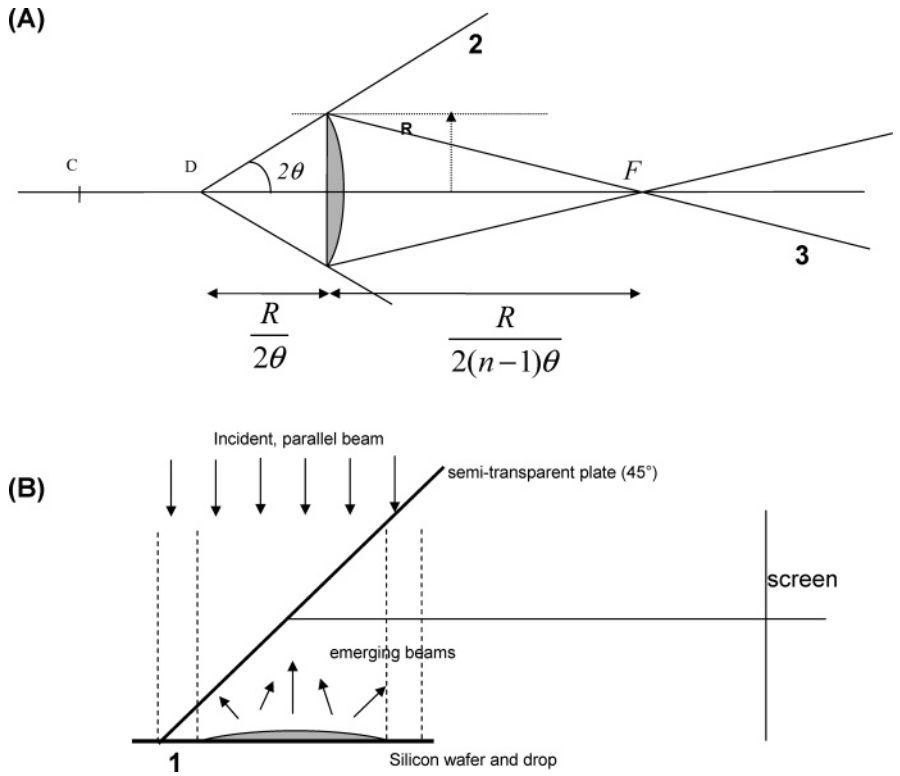

Figure 2. Schematic view of the optical setup (not to scale, the angles are in fact very small). (A) Definition of the emerging beams: C is the geometrical center of the drop when it is a spherical cap, located at R/q from the substrate. The emerging beam (2) is reflected on the drop surface and seems to come from point D, located at $R/2q$. The beam (3) has crossed the drop twice and converges at point F on the axis. (B) Geometry of the setup.

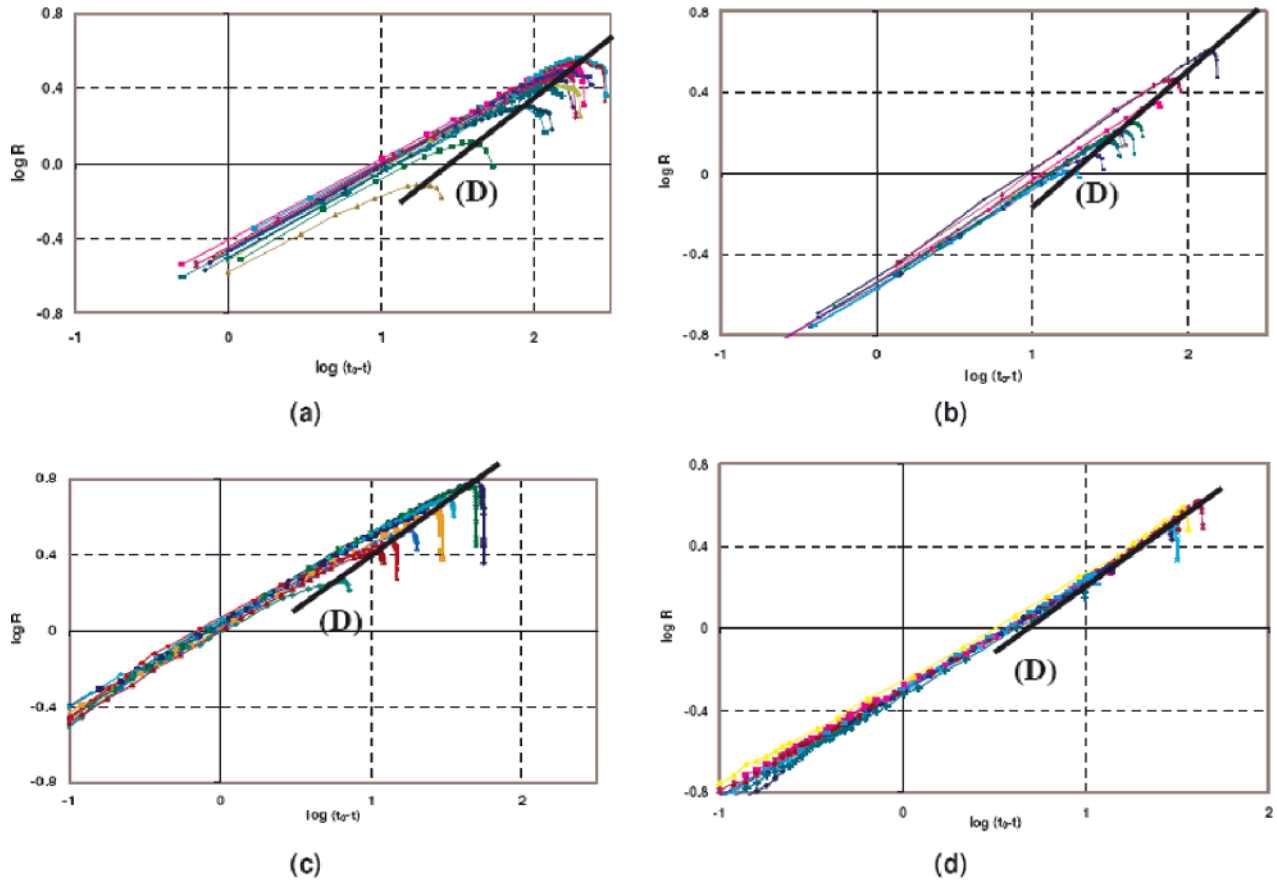

Figure 3. Log−log plot of the radius R versus time $(t_0 - t)$ for different initial volumes of alkane droplets. The line D passes by maximum radii for each volume. (a) Nonane: the measured slope of D is 0.64. (b) Octane: the measured slope of D is 0.64. (c) Heptane: the measured slope of D is 0.63. (d) Hexane: the measured slope of D is 0.63.

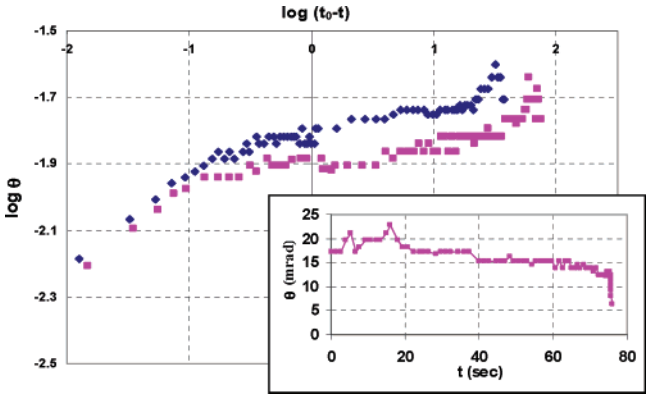

Figure 4. Log−log plot of the contact angle θ versus time ($t_0 - t$) for different initial volumes of heptane droplets: (◆) 3 μL and (■) 10 μL. (Inset) Linear representation of the contact angle versus time (3 μL).

3c), and hexane (3d) are plotted versus the time interval $t_0 - t$ for different values of the initial drop volume, both in the advancing and receding motion. The range of volumes investigated is much larger than in the previous studies;[17−19] therefore, it becomes clear that the receding part of the various curves do not superimpose exactly, contrary to our previous conclusions. The locus of the extrema in the log−log plot is a straight line with slope ~0.64, the same for the four alkanes investigated.

In the second series of figures, the contact angles θ measured under a microscope are plotted versus the time interval for two different volumes of heptane drops. As previously explained, measuring the contact angle of an evaporating drop is difficult. Moreover, the noise on the data is accentuated by the log−log representation (Figure 4a), because the angles are close to 0. The oscillations in the vicinity of the maximum extension of the drop are very reproducible and not because of any air draft; they are more visible on the linear plot (Figure 4b). As previously mentioned, there is a steep decrease of the contact angle during the spreading and the beginning of the retraction, then at a range where the contact angle is almost constant, and where the relation $2y + x = 1$ is obeyed. Finally, there is again a fast decrease at the end of the drop. The log−log curves for the two volumes are shifted in the main part and tend to merge at the end.

The second setup allows us to compare the results obtained with the different masks (Figure 5). The straight lines on parts a and b of Figure 5 have the slope $y - x$, which is expected for the ratio R/θ if the drop is a spherical cap.

The drop shape can be distorted by (i) gravity and (ii) surface-tension gradients. (i) As far as gravity is concerned, the maximum radius of the biggest drops is larger than the capillary length $a = \sqrt{\gamma / \rho g}$ ($a \approx 1.8$ mm), which means that these drops will be flatter than spherical. Let us give an estimate of the flattening of the drop. In the lubrication approximation, the static, three-dimensional drop profile is given by the equation

$$-\left(\frac{d^2h}{dr^2} + \frac{1}{r}\frac{dh}{dr}\right) = K_E - \frac{\rho g}{\gamma}h \qquad (1)$$

Here, γ is the surface tension; ρ is the density; g is the acceleration of gravity; h is the local thickness; and K_E is the curvature at the contact line, which is simply $2\theta/R$ for spherical caps. For flattened drops, the two radius of curvatures are the same at the center ($r = 0$) but no longer at the edge ($r = R$). The present experiment measures R/θ

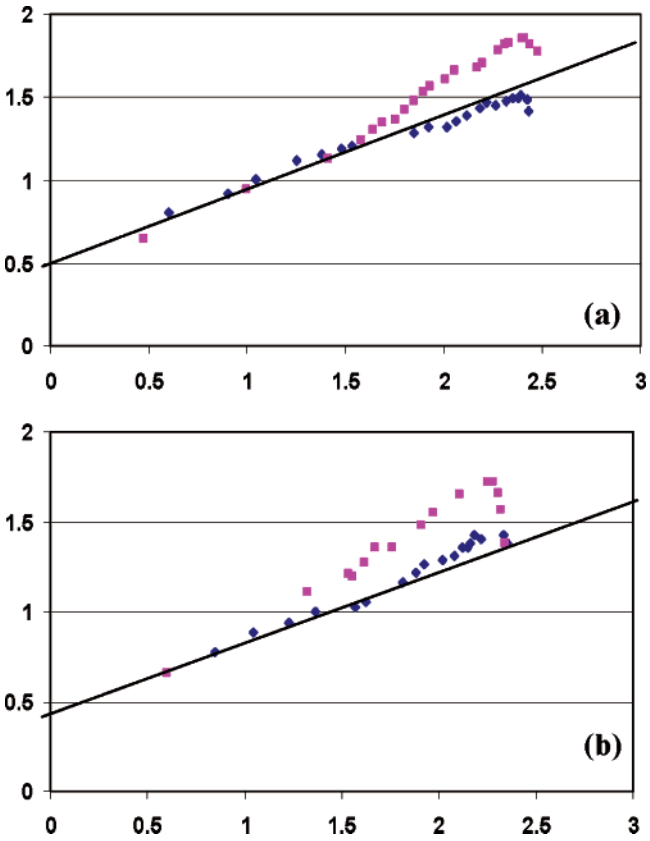

Figure 5. Log−log plot of the radius of curvature (cm) versus $t_0 - t$ (s) for a drop of octane with a maximum radius of 5 mm and two different initial volumes: 4 μL (a) and 7 μL (b). (◆) R/θ, which is on the radius of curvature at the contact line. (■) $(-d^2h/dr^2)_{r=0}^{-1}$, which is the radius of curvature at the center. The slope of the straight line in the two cases is $y - x \approx 0.4$.

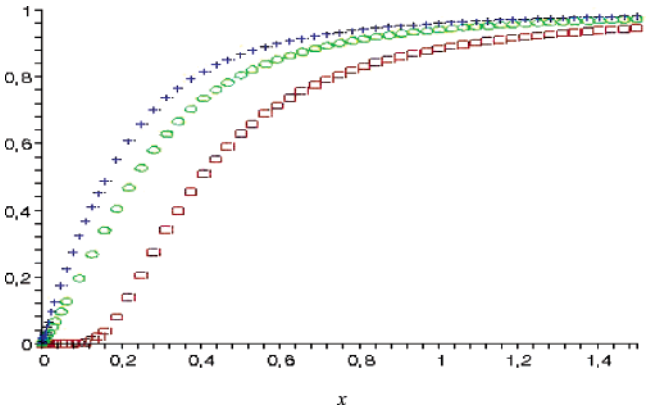

Figure 6. Comparison between the parameters of the flattened drop and the flattened drops of a spherical cap with the same radius and contact angle $\theta = 0.012$ rad, as a function of $x = a/R$. (+) Ratio of the volumes. (○) Ratio of the heights. (□) Ratio of the curvatures in a plane of symmetry of the drop: $(-d^2h/dr^2)_{r=0}^{-1}$ (curvature at the center) and θ/R (curvature at the edge).

at the edge and $(-d^2h/dr^2)_{r=0}^{-1} = \lim(r \to 0)\, r(dh/dr)_{r \to 0}^{-1}$ at the center.

Solving eq 1 for a given contact angle allows us to calculate the various parameters as a function of the ratio a/R and to compare them with the ones of a spherical cap with the same contact angle and radius. The value of the contact angle is chosen to be $\theta = 0.012$ rad, which is typical of octane. Then, eq 1 is solved with $K_E = 2\theta/R$.

On Figure 6, the ratios of the curvatures, the drop heights, and the drop volumes have been plotted as a

function of a/R for $\theta = 0.012$ rad. The curvature is the most sensitive parameter, and the calculations are in good agreement with the measurements on Figure 5. The fact that the lines with slope $y - x$ fit the data at the contact line even for flattened drops means that the volume of these drops is not yet significantly different from the ones of spherical caps with the same R and θ, as can be seen also in the figure. It would no longer be the case for larger drops.

(ii) Surface-tension gradients can be induced by evaporation. They are directed outward if the edge of the drop is colder, which is the case during spreading[29−30] and then flatten the drop. They fade out when the drop has reached its maximum extension and stays some time there at a constant radius, while the contact angle decreases with oscillations superimposed. No evidence of gradients during retraction can be inferred from the drop profile, because the mere gravity is enough to account for the observed shape.

The conclusion is that, for the alkanes considered, small drops, i.e., with radius of the order of the capillary length or less, are spherical caps, while larger ones are flatter. Including gravity allows us to account for the observations, without introducing any surface-tension gradient (which does not mean that there is no gradient, only that they play as higher order terms). Moreover, the incidence of gravity on the dynamics seems to be weak, in the range of drop sizes investigated.

One must be aware that evaporation takes place during spreading as well and that the volume of the drop when it starts to recede is much smaller than the initial volume. From the measured contact angle and radius, we can estimate the volume of the drop at the beginning of retraction, a value which is slightly overestimated if the drop is flatter than spherical, because we use the contact angle measured with the microscope. The volume of the drop at the maximum extension is approximately 35% of the initial volume for nonane, 30% for octane, 25% for heptane, and 15% for hexane. Therefore, we refrain to propose models for the curves on Figure 1.

3. Theoretical Analysis: Rescaling

The starting point for the evolution of the drop is the local conservation equation

$$\frac{\partial h}{\partial t} + \nabla(hU) = -J(r) \tag{2}$$

Here, h is the local thickness; r is the distance to the drop axis; η is the viscosity of the alkane; and U is the velocity averaged over the thickness.

$$U(h,t) = \frac{h^2}{3\eta}\nabla(\gamma\Delta h - \rho g h + \Pi(h)) + \frac{h}{2\eta}\nabla\gamma \tag{3}$$

$J(r)$ is the evaporation rate per unit area of the substrate, and $\Pi(h)$ is the disjoining pressure. When surface-tension gradients are ignored, which is supported by the previous discussion, one gets

$$U(h,t) = \frac{h^2\gamma}{3\eta}\nabla\left(\Delta h - \frac{h}{a^2} + \frac{\Pi(h)}{\gamma}\right) \tag{4}$$

where $a = \sqrt{\gamma / \rho g}$ is the capillary length.

With the assumption of a diffusion-controlled, quasi-stationary evaporation process and considering that the contact angles are very small, the evaporation rate can be written as[14,20−21]

$$J(r) = \frac{j_0}{R\sqrt{1 - \left(\frac{r}{R}\right)^2}} \tag{5}$$

where R is again the radius of the drop. Equation 5 is deduced from an electrostatic analogy with a flat disk kept at constant potential. In a macroscopic description, the electric field (or the evaporation rate) diverges at the edge of the drop. A specific discussion at the proper scale will be needed when the behavior of the contact line is explicitly discussed.

Equation 2 is conveniently rescaled using characteristic lengths and times. A characteristic length should be some radius, which from the experimental study can be chosen as the maximum radius of the drop R_0. A characteristic thickness in the lubrication approximation is $R_0\theta_0$, where θ_0 is logically the angle corresponding to R_0 taken at the beginning of the retraction. The characteristic time is then $R_0^2\theta_0/j_0$.

Let us now proceed with the equation. Rescaling introduces several dimensionless quantities

$$C = 3\eta j_0/\gamma R_0\theta_0^4 \text{ is a capillary number}$$

The influence of the gravity is contained in the Bond number

$$\alpha = \frac{R_0^2}{a^2}$$

The disjoining pressure will play at the edge of the drop. Let us assume pure van der Waals interaction, and let H be the absolute value of the Hamaker constant. The disjoining pressure is positive in complete wetting and can be written as

$$\Pi(h) = \frac{H}{6\pi h^3}$$

The second dimensionless quantity is a "van der Waals" number

$$A = \frac{H}{6\pi\gamma R_0^2\theta_0^4}$$

The equation becomes, keeping the same symbols for the dimensionless variables

$$\frac{\partial h}{\partial t} + \frac{1}{C}\nabla\left(h^3\nabla\left(\Delta h - \alpha h + \frac{A}{h^3}\right)\right) = -\frac{1}{R\sqrt{1 - \left(\frac{r}{R}\right)^2}} \tag{6}$$

A is very small, but C and α are of the order 1. For example, $C = 0.16$ and $\alpha = 4$ for a 3 μL drop of heptane, where $R_0 = 3.6$ mm. The same orders of magnitude are obtained with the other alkanes.

Rescaling: Check against Experiments. The relevance of the rescaling can be checked easily on the experimental log−log plots, because it corresponds to a mere translation such that the curves coincide at the maximum extension.

For a given alkane, the curves for the radius merge very well if they are translated parallel to the line with

(29) Redon, C.; Brochard-Wyart, F.; Rondelez, F. *J. Phys. II* **1992**, *2*, 580.

(30) Bénichou, O.; Cachile, M.; Cazabat, A. M.; Poulard, C.; Valignat, M. P.; Vandenbrouck, F.; van Effenterre, D. *Adv. Colloid Interface Sci.* **2003**, *100−102*, 381.

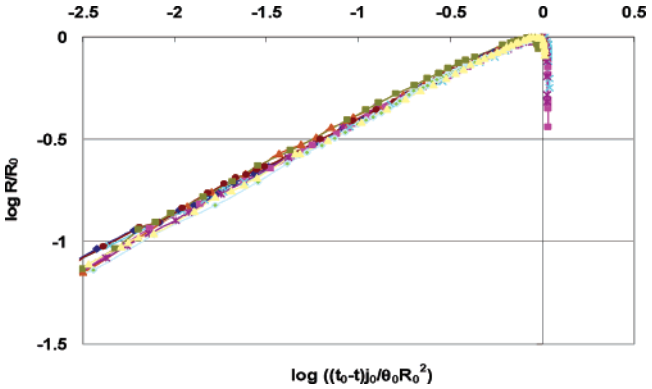

Figure 7. Log−log plot of the rescaled radius versus the rescaled time for different initial volumes of heptane droplets.

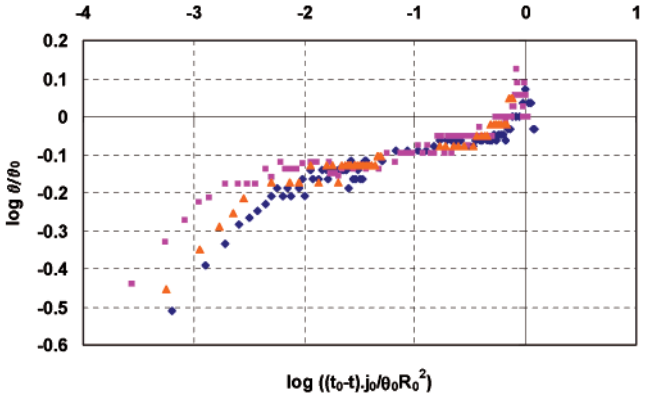

Figure 8. Log−log plot of the rescaled contact angle versus the rescaled time for different initial volumes of heptane droplets: (◆) 3 μL, (▲) 5 μL, and (■) 10 μL.

slope 0.64. A true rescaling has been done for heptane, where precise measurements of the angle are available, and works very well (see Figure 7).

For the angle, the rescaling works also, except at the very end of the drop, where the decrease of the angle is faster (see Figure 8).

Note that R_0 and θ_0 are not independent quantities. From direct measurements in heptane, the trend is that $\theta_0 \propto R_0^z$, with $z \approx -0.4$. The shifts needed to superimpose the curves for the radius in the log−log plot gives the best estimate. Here, the vertical shift is log R_0; the horizontal one is log $\theta_0 R_0^2$; and the slope is -0.63, which gives $z = -0.45$ (see Figure 3).

In conclusion, the rescaling works well, except at the very end of the drop. It is clear from Figure 4 that, in that range, the curves for the contact angle have a tendency to merge before scaling but not after, which deserves further discussion.

One obvious explanation for the faster decrease of the angle at the end of the drop is that the velocity becomes large there, which in a receding motion reduces the angle. This is true, but this effect is already taken into account in the hydrodynamic term and therefore properly rescaled.

On the other hand, one must be aware that the rescaling in time depends directly on the structure of the evaporation term, i.e.

$$J(r) \propto \frac{j_0}{R} \tag{7}$$

which means that the rate of change of the volume V of a drop with small contact angle is proportional to the radius R

$$\frac{dV}{dt} \propto R \tag{8}$$

If the drop is a spherical cap and if power laws for the radius and angle versus $t_0 - t$ are still observed, the corresponding exponents y and x have to be linked by $2y + x = 1$.

Experiments show that the drops keep a perfect spherical cap shape until the very end.[19] In that range, the fit with a power law is excellent for the radius with no appreciable change in y ($y \sim 0.5$). The uncertainty is larger for the angle (Figure 4); however, the data are acceptably fitted by a power law, where $x \sim 0.4-0.5$, in sharp disagreement with the relation $2y + x = 1$. This suggests that eq 7 is not valid at the end of the drop life.

The change in evaporation rate suggests that the assumption of a diffusion-controlled, quasistationary evaporation process does not hold at the end of the drop.

This can be due to the large interface velocity, which could induce convection in the gas phase.[18]

Another explanation would be that eq 5 is no longer valid for drops of microscopic thickness. Because the fast decrease of the angle is already visible for relatively thick drops (1 μm), the experiment suggests that convection is the most plausible explanation.

Whatever the cause of the change in the evaporation rate, the rescaling has to be done accordingly. This could possibly explain why the contact angle seems to depend only weakly on the drop volume at the very end of the drop's life.

We shall restrict the discussion to the range where eq 7 is valid.

4. Theoretical Analysis: Regularization

To address the dynamics of the moving contact line, the evaporation rate at the edge of the drop needs to be discussed at the proper, i.e., microscopic scale, where the flux is finite.

Two approaches may be proposed. First, the assumption of a diffusion-controlled, quasistationary evaporation process could be reconsidered at the edge. A generalized boundary condition at the liquid/gas interface has been derived in ref 33. A possible regularization is then to make the evaporation flux saturate at a distance $l = D/v_{th}$ from the periphery of the drop (D is the diffusivity of the vapor in air, and v_{th} is a typical thermal velocity).

Second, the rate of evaporation of thin wetting films depends on the film thickness and tends to 0 with it (from that point of view, eq 6 is not correct, because the disjoining pressure should also appear in the right-hand side). Therefore, the evaporation rate will saturate at some distance l from the edge of the drop, where the film becomes thin and the disjoining pressure comes into play.

Let us develop the approach based on the specific properties of thin films. Let $x = R - r$ be the (rescaled) distance from the edge ($x > 0$). In the frame of the contact line, which moves with velocity dR/dt and for $x \ll 1$, the eq 6 can be written as

(31) de Gennes, P. G.; Hervet, H. Dynamique du mouillage: Films précurseurs sur solide sec. *C. R. Acad. Sci. Paris* **1984**, *299*, 499.
(32) Jackson, J. D. *Classical Electrodynamics*, 2nd ed.; Wiley: New York, 1975.
(33) Sultan, E.; Boudaoud, A.; Ben Amar, M. Evaporation of a thin film: Diffusion of the vapour and Marangoni instabilities. *J. Fluid Mech.* **2005**, manuscript submitted.

$$\frac{dR}{dt}\frac{\partial h}{\partial x} + \frac{1}{C}\frac{\partial}{\partial x}\left(h^3\frac{\partial}{\partial x}\left(\frac{\partial^2}{\partial x^2}h + \frac{A}{h^3}\right)\right) = -\frac{1}{\sqrt{2Rx}} \quad (9)$$

We first look for a power-law form for the profile of the drop near the edge. It appears that the most divergent terms come from capillarity and van der Waals forces so that advection and evaporation are negligible near the contact line. The profile at the edge is given by

$$\frac{\partial^2}{\partial x^2}h + \frac{A}{h^3} = 0 \quad \text{which leads to} \quad h = A^{1/4}\sqrt{2x}$$

This is the same result as the one obtained by de Gennes and Hervet[31] for the edge of the precursor film in complete wetting. The crossover to the main drop ($h = \theta x$) with contact angle θ takes place over a distance $l \approx A^{1/2}/\theta^2$. This distance l gives the macroscopic edge of the drop.

To find the macroscopic behavior of the drop, we come back to eq 9. Then, van der Waals forces become subdominant and can be neglected. All other terms should match at the crossover distance l

$$\frac{dR}{dt} - \frac{1}{C}\theta^3 \approx -\frac{1}{2^{1/2}A^{1/4}\sqrt{R}} \quad (10)$$

up to numerical factors of the order 1. This equation is a generalization of Tanner's law[34] accounting for evaporation.

In the range where the drops are spherical caps, volume conservation yields

$$3R\theta\frac{dR}{dt} + R^2\frac{d\theta}{dt} = -8 \quad (11)$$

This closed system (eqs 10 and 11) for the radius and the contact can be solved numerically (see the next section).

One obvious limitation of the derivation of the mobility law for the contact line is that it is valid as long as $l \ll R$, a condition which is broken at the end of the drop life.

Note that if one makes the evaporation flux saturate at a distance $l = D/v_{th}$ from the periphery of the drop, one gets a slightly different mobility law

$$\frac{dR}{dt} - \frac{1}{C}\theta^3 \approx -\frac{1}{\theta\sqrt{lR}} \quad (12)$$

Check Against Experiments. The relevance of the regularization procedure can be indirectly checked on eq 10. At the maximum extension, the rescaled R and θ are equal to 1 and the velocity $dR/dt = 0$. Therefore

$$C = 2^{1/2}A^{1/4} \quad (13)$$

Coming back to the usual variables, one finds a relation between θ_0 and R_0

$$\theta_0^3 = \frac{3\eta j_0}{\gamma}\left(\frac{4H}{6\pi\gamma}\right)^{-1/4}\frac{1}{\sqrt{R_0}} \quad (14)$$

The orders of magnitude are correct, but the relation between the angle and radius at the maximum differs significantly from the experimental power law $\theta_0 \propto R_0^{-0.45}$. This could be expected, because the regularization has been done using an oversimplified procedure. However, the mere fact to be able to find a relation between maximum radius and angle is already a significant step toward the complete description of the evaporating wedge.

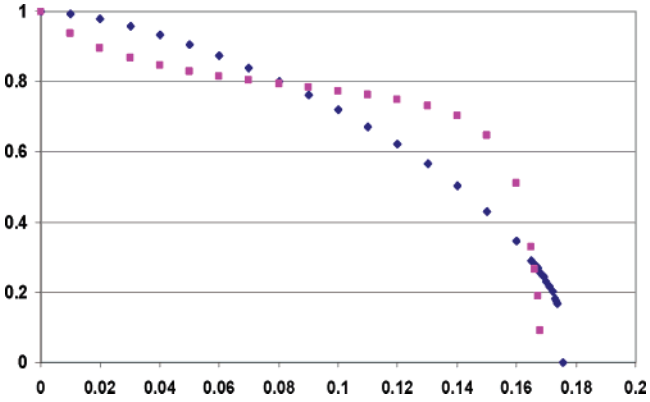

Figure 9. Calculated rescaled contact angle θ (■) and radius R (◆) versus the rescaled time t.

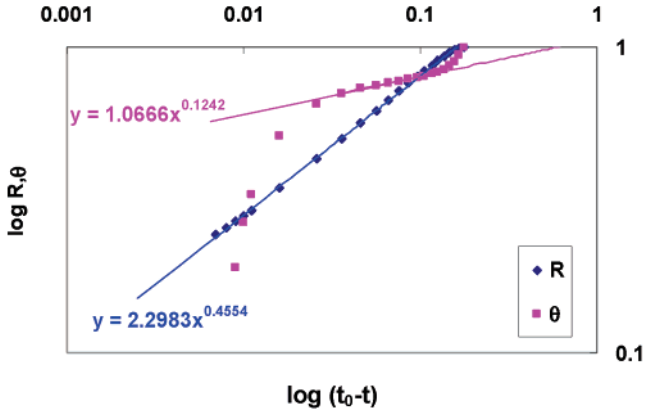

Figure 10. Log−log plot of the rescaled contact angle θ and radius R versus the rescaled time ($t_0 - t$).

The coupled eqs 10 and 11 can be solved numerically, taking the maximum extension as the initial condition, with $R = 1$, $\theta = 1$, and $dR/dt = 0$, which implies that eq 13 is valid. Therefore, the only free parameter is C. When the experimental value $C = 0.16$ is used, one obtains the curves plotted on Figure 9. The agreement is qualitatively excellent. Quantitatively, the results are very sensitive to the value of C, which is not fully plausible. Moreover, the angle vanishes before the radius and diverges toward $-\infty$. This behavior is reminiscent of the inadequacy of the wedge model in partial wetting at large receding velocities.[35] Because eq 10 is no longer valid at small R ($R \approx l$), how to define t_0 precisely is not obvious. An extrapolation of the data at $R \gg l$ has been used, allowing us to obtain the log−log plots reported on Figure 10.

A numerical solution of the system (eqs 11 and 12) has also been calculated. The results are quite similar, except for a slight shift in the values of the parameter C.

5. Conclusion

It is clear that the present theory picks up a large part of the physics of the problem and represents a significant step toward its complete understanding. It accounts well for the experimental power laws obtained for the radius of receding, evaporating drops. It also provides the first attempt to predict the value of the contact angle in a dynamic situation and a generalization of Tanner's law in the case of evaporating liquids. It has to be improved

(34) Tanner, L. H. *J. Phys. D* **1979**, *12*, 1478.

(35) Cox, R. G. *J. Fluid Mech.* **1986**, *168*, 169.

at some places. Noticeably, the sensitivity of the solution to the value of C, i.e., to the hydrodynamic term, has to be smoothed out, which means that a real profile has to be introduced in the equations and not only the slope at the edge. However, it provides the first complete and plausible description of the very old problem of evaporation of drops on solid substrates.

Acknowledgment. We gratefully acknowledge M. Brenner, H. Stone, and M. Betterton, who gave access to unpublished work, and Elie Raphaël for enlightening discussions. Sergueï Mechkkov and Baptiste Mangeney took part in some of the experiments.

LA050406V